[5]Fertig, M., Fruhauf, H. H., and Auweter-Kurtz, M., "Modelling of Reactive Processes at SiC Surfaces in Rarefied Nonequilibrium Airflows," AIAA Paper 2002-3102, June 2002.

[6]Armenise, I., Capitelli, M., Colonna, G., Koudriavtsev, N., and Smetanin, V., "Nonequilibrium Vibrational Kinetics During Hypersonic Flow of a Solid Body in Nitrogen and Its Influence on the Surface Heat Flux," *Plasma Chemistry and Plasma Processing*, Vol. 15, No. 3, 1995, pp. 501–528.

[7]Capitelli, M., Armenise, I., and Gorse, C., "State-to-State Approach in the Kinetics of Air Components Under Re-Entry Conditions," *Journal of Thermophysics and Heat Transfer*, Vol. 11, No. 4, 1997, pp. 570–578.

B. Hassan
Associate Editor

International Space Station Ku-Band Communications Antenna Blockage Analysis

Shian U. Hwu* and Yin-Chung Loh†
Lockheed Martin Space Operations, Houston, Texas 77258
and
Quin D. Kroll‡ and Catherine C. Sham§
NASA Johnson Space Center, Houston, Texas 77258

Introduction

THE International Space Station (ISS) is a large and complex spacecraft. The solar panels and thermal radiators are rotated dynamically to maintain a preferential orientation with respect to the sun. The space station Ku-band antenna tracks the geostationary Tracking Data and Relay Satellite (TDRS) and will encounter blockage from the space station structures, especially the solar panels and the thermal radiators, as shown in Fig. 1. These blockages may cause communication outages and reduce communication quality. An understanding of blockage effects is necessary for prediction of communication coverage. The ISS Ku-band antenna is a 2-m-diam reflector antenna. The antenna's operating frequencies are 15.0034 GHz for transmitting and 13.775 GHz for receiving. The previous ISS Ku-band antenna model for communication coverage analysis is very conservative.[1] This conservative approach is based on International Space Station/Shuttle reflector antenna test data. Additional computer simulation and test results indicate that in the near field, the energy radiated by the reflector antenna is mostly confined within the antenna aperture projected cylinder.[2] The Ku-band communication link was assumed to be lost if the 2-m-aperture projected cylinder was blocked by any ISS structures. If the antenna's aperture projected cylinder is clear of any structure blockage, the multipath degradation from ISS structures is insignificant. The communication link will not be subject to much impact from the ISS structure multipath effects.

Recently obtained uplink flight data indicate that the 2-m-diam cylinder model is too conservative.[1] Flight data indicate that the Ku-band antenna can track the TDRS satellite with partial solar panel or thermal radiator blockage. The data indicate that the ISS Ku-band link can sustain 4.6 dB signal-power-level degradation (relative to the signal power without structure blockage at maximum slant range to TDRS) before the software controller forces the communication link to drop. As a result of the 4.6-dB available margin, partial blockage to the ISS Ku-band reflector antenna should be allowed in the Ku-band communication coverage analysis to better reflect the actual communication link margin and coverage performance. The following simulation and analysis were performed to improve the previously used conservative approach to better predict the actual communication performance.

Signal Strength Computations

In the communication system performance simulations, the ISS Ku-band reflector antenna is modeled by a set of equivalent dipoles. The reflector antenna aperture fields are computed and then converted to a set of equivalent dipoles. The equivalent dipoles are used as the equivalent radiation sources of the ISS Ku-band reflector antenna. The solar panels and thermal radiators are modeled as perfect conducting plates. The solar array panel is a composite structure formed by closely spaced solar cells. The solar cells are made of silicon and are welded onto the front surface of the solar array panel. A grid of copper strips that collect current is on the back side of the solar array panel. To characterize the scattering properties of the solar array panels, experimental investigations were performed at Ku-band frequencies. Based on the results obtained, the solar array panels exhibit scattering properties similar to those of a conducting panel of the same size.[1] The solar array panels were modeled approximately using perfect reflecting plates at Ku-band frequencies.

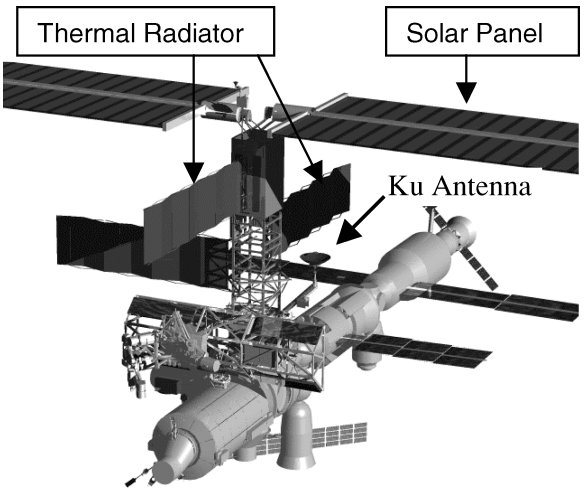

Fig. 1 Ku-band antenna will encounter solar panel and thermal radiator blockage.

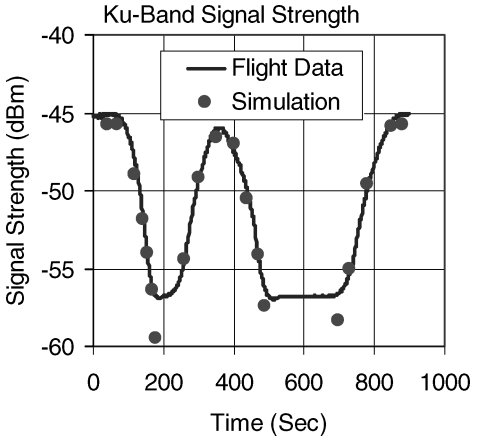

Fig. 2 Computed signal strength compared with flight data along a selected TDRS satellite path with solar panel blockage.

Received 14 April 2003; revision received 16 December 2003; accepted for publication 16 December 2003.

*Senior Staff Engineer, Avionics Systems Analysis Section, 2400 NASA Road 1. Senior Member AIAA.

†Section Manager, Avionics Systems Analysis Section.

‡Project Engineer, Systems Analysis and Verification Branch, MC: EV7, 2101 NASA Road 1.

§Deputy Branch Chief, Systems Analysis and Verification Branch, MC: EV7, 2101 NASA Road 1.

Two-meter gaps between solar panels were incorporated into the model.

The simulation data are computed using the geometrical theory of diffraction (GTD).[3,4] The signal strengths are computed by summing up all the individual dipole antenna patterns with solar panel and thermal radiator blockages. The reflected and diffracted field at a field point r', $\boldsymbol{E}^{r,d}(r')$, can be computed as

$$\boldsymbol{E}^{r,d}(r') = \boldsymbol{E}^{i}(r)\boldsymbol{D}^{r,d}\boldsymbol{A}^{r,d}(s)e^{-jks} \tag{1}$$

where $\boldsymbol{E}^{i}(r)$ is the field incident on the reflection or diffraction point r, $\boldsymbol{D}^{r,d}$ is a dyadic reflection or diffraction coefficient, $\boldsymbol{A}^{r,d}(s)$ is a spreading factor, and s is the distance from the reflection or diffraction point r to the field point r'. $\boldsymbol{D}^{r,d}$ and $\boldsymbol{A}^{r,d}$ can be found from the geometry of the structure at the reflection or diffraction point r and the properties of the incident wave there.

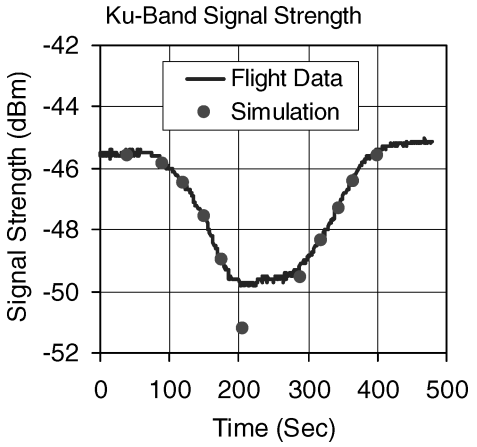

Fig. 3 Computed signal strength compared with flight data along a selected TDRS satellite path with thermal radiator blockage.

Comparison of Flight Data and Simulation Results

Both measured and computed results indicate that the level of signal strength degradation from solar panel and thermal radiator structure blockage is mainly a function of antenna aperture blockage. The other secondary factors are antenna pointing direction, structure size and shape, structure material, structure orientation, separation distance, and surface roughness. The antenna's gain reduction, pattern distortion, and boresight tilt are results of the partial solar panel and thermal radiator blockage of the antenna.

The computed ISS Ku-band signal strengths using GTD along selected TDRS satellite paths with solar panel or thermal radiator blockage are shown in Figs. 2 and 3. To validate the GTD computed results, uplink flight data are shown for comparison. The flight data are the International Space Station Ku-band receiver intermediate frequency tracking signal power level. The accuracy is within 0.5 dB, based on the system design requirement verification data. Figure 4 shows the selected TDRS satellite path, which is also the Ku-band antenna pointing path, because the antenna tracks the TDRS satellite. The Ku-band antenna encountered solar panel blockage along this path. The rectangular shading regions shown in Fig. 4 are the software masks to protect sensitive equipment from antenna radiations. Figure 2 shows GTD computed signal strength compared with uplink flight data along the selected TDRS satellite path with solar panel blockage. Figure 5 shows a selected TDRS satellite path with thermal radiator blockage. The Ku-band antenna encountered thermal radiator blockage along this path. Figure 3 shows computed signal strength compared with uplink flight data along the selected TDRS satellite path with thermal radiator blockage.

Good agreement is observed between flight data and GTD computed results. Both flight data and simulation results indicate that

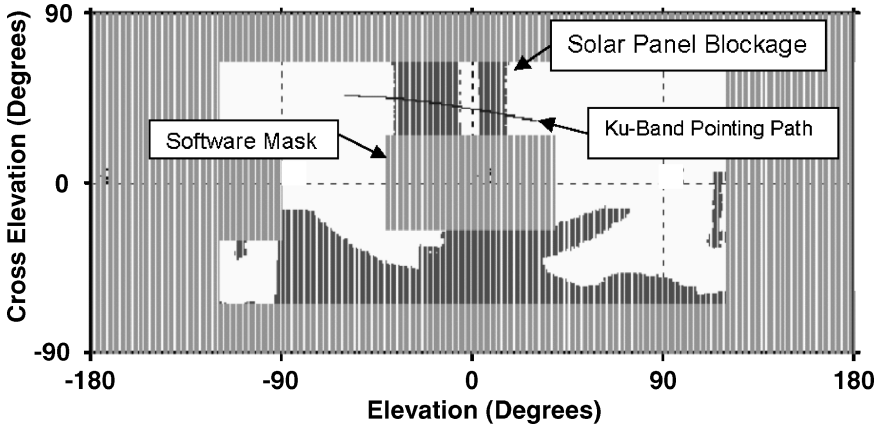

Fig. 4 Selected TDRS satellite path (Ku-band antenna pointing path) with solar panel blockage.

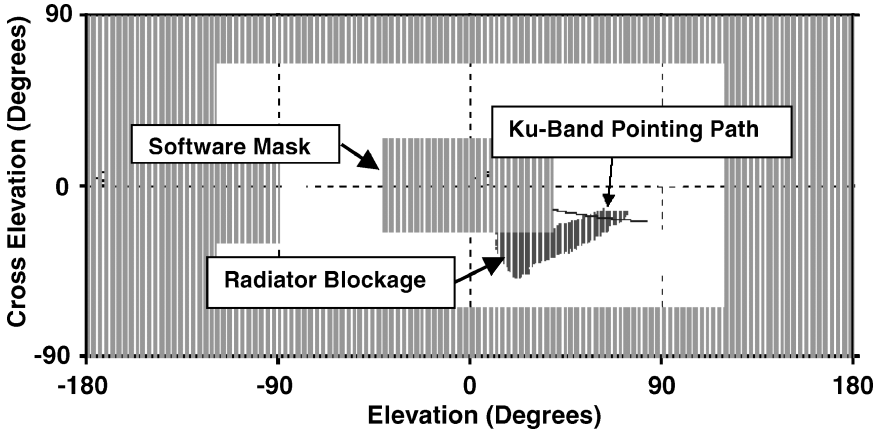

Fig. 5 Selected TDRS satellite path (Ku-band antenna pointing path) with thermal radiator blockage.

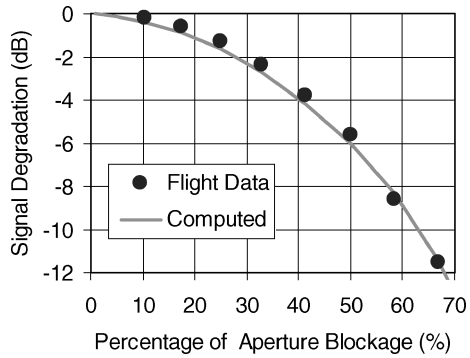

Fig. 6 Signal strength reduction as a function of percentage of ISS Ku-band antenna aperture blockage.

the signal strength decreases as the structure penetraties the antenna aperture projected cylinder. The gain reduction is mainly due to decreasing aperture area or effective antenna size and can be estimated based on the aperture blockage area, as shown in Fig. 6, derived from averaging the solar panel and radiator blockage results. Another factor causing gain reduction is the shift of the antenna main beam pattern (sum and difference patterns). However, it is not significant enough to impact the ISS antenna autotracking performance.

As shown in Figs. 2 and 3, the flight data reach a floor value of about −57 dBm. The simulation results actually decrease even further, depending on the size of the remaining unblocked aperture area. The signal strength increases after structure blockage of the antenna aperture projected cylinder ceases. The computed results, in general, predict a deeper null caused by the solar panel blockage. This is expected because the solar panel was modeled as a perfect conducting plate in the simulations. The actual solar array panel is a composite structure formed by closely spaced solar cells. The flight data indicate that the Ku band can withstand 4.6-dB degradation and still maintain the data flow. The GTD simulations indicate that a 4.6-dB degradation corresponds to about 40% aperture blockage. The ISS Ku-band communication link will be considered lost if more than 40% of the aperture projected cylinder is blocked by ISS structures.

Conclusions

The ISS Ku-band antenna model for communication coverage analysis[1] is updated and validated using recently obtained flight data. The flight data indicate the ISS Ku-band link can sustain 4.6-dB degradation from structure blockage. The updated antenna model for the ISS Ku-band reflector antenna, based on the flight data and GTD simulations, allows up to 40% structure blockage of the antenna aperture before declaring Ku-band communication outages. The communication coverage based on the updated antenna model reflects the actual Ku-band link margin and antenna performance. A better match in the communication coverage is achieved between computer simulations and actual measurements.

References

[1]Hwu, S. U., Lu, B. P., Johnson, L. A., Fournet, J. S., Panneton, R. J., and Arndt, G. D., "Scattering Properties of Solar Panels for Antenna Pattern Analysis," *Proceedings of IEEE International Antennas and Propagation Symposium & URSI Radio Science Meeting*, Inst. of Electrical and Electronics Engineers, Piscataway, NJ, 1994, pp. 266–269.

[2]Lewis, R. L., and Newell, A. C., "Efficient and Accurate Method for Calculating and Representing Power Density in the Near Zone of Microwave Antennas," *IEEE Transactions on Antennas and Propagation*, Vol. 36, No. 6, 1988, pp. 890–901.

[3]Kouyoumijian, R. G., and Pathak, P. H., "A Uniform Geometrical Theory of Diffraction for an Edge in a Perfectly Conducting Surface," *Proceedings of IEEE*, Vol. 62, No. 11, 1974, pp. 1448–1461.

[4]Marhefka, R. J., and Silvestro, J. W., "Near Zone—Basic Scattering Code User's Manual with Space Station Applications," NASA CR-181944, Dec. 1989.

N. Gatsonis
Associate Editor

Optimal Control of Tethered Planetary Capture Missions

Paul Williams*
Royal Melbourne Institute of Technology, Melbourne, Victoria 3001, Australia

Nomenclature

A	=	tether cross-sectional area, m^2
a	=	semimajor axis of orbit, m
e	=	orbit eccentricity
F	=	factor of safety for tether material, 1.5
f	=	orbit true anomaly of the tether system center of mass, rad
g	=	gravitational acceleration at Earth sea level, 9.81 m/s^2
I_{sp}	=	specific impulse of chemical propellant, s
L	=	tether reference length, m
l	=	tether length, m
m	=	total system mass, $m_1 + m_2 + m_t$, kg
m_t	=	deployed tether mass, ρAl, kg
m_1	=	mass of main spacecraft, kg
m_2	=	mass of payload, kg
m^*	=	reduced system mass, kg
R	=	orbit radius to the system center of mass, m
R_p	=	periapsis radius of approach hyperbolic orbit, m
T	=	tether control tension, N
u	=	nondimensional control tension, $T/[m_1 \dot{f}^2 L(m_2 + m_t)/m]$
v_∞	=	hyperbolic approach velocity, m/s
θ	=	in-plane tether libration angle, rad
Λ	=	nondimensional tether length, l/L
μ	=	gravitational constant of central planet, km^3/s^2
ρ	=	tether mass density, kg/m^3
σ_{ut}	=	ultimate tensile strength of tether material, N/m^2

Superscripts

$\cdot$	=	differentiation with respect to time, d( )/dt
$'$	=	differentiation with respect to orbit true anomaly, d( )/df

Introduction

TETHERED spacecraft have been proposed for a wide variety of advanced space applications, both in the vicinity of the Earth and in interplanetary missions.[1] A new application of tethers in interplanetary spaceflight, first mentioned by Longuski et al.,[2] has been further investigated by Williams et al.[3,4] In this application, called tethered planetary capture, a tethered payload is deployed from a mother spacecraft while the system is on a hyperbolic flyby trajectory of a target planet. The basic maneuver is depicted in Fig. 1, which shows the following: 1) The payload is deployed via a tether in a hyperbolic approach orbit and made to spin or swing in the positive direction indicted in Fig. 1. 2) The payload is released from the tether at an appropriate moment so that it is captured into an elliptical orbit. 3) The main spacecraft gains an additional boost and is sent on a new escape trajectory. By suitable selection of system parameters, such as tether length and spin rate, it is possible to achieve planetary capture without expending any chemical propellant.

The dynamics of the tethered planetary capture maneuver, as well as preliminary control schemes were presented by Williams et al.[3,4]

Received 10 September 2003; revision received 13 December 2003; accepted for publication 15 December 2003.

*Ph.D. Candidate, Department of Aerospace Engineering, G.P.O. Box 2476V; tethers@hotmail.com. Student Member AIAA.